# Potential Military Cotton Textiles by Carbon Quantum Dots

**Hossam E. Emam**
National Research Centre
**Mahmoud El-Shahat**
National Research Centre
**Mohamed S. Hasanin**
National Research Centre
**Hanan B. Ahmed** ( hananbasiony@gmail.com )
Helwan University Faculty of Science

**Research Article**

**Keywords:** Pyrimidine based heterocycle, CQDs, Cationized cotton, Fluorescence, UV-protection, Anti-microbe, Durability.

**Posted Date:** April 28th, 2021

**DOI:** https://doi.org/10.21203/rs.3.rs-411549/v1

# Abstract

Owing to the sensitivity for color vicissitude by exposing to UV irradiation, manufacturing of fluorescent fabrics is widely demanded to be exploited in camping, sensing and military purposes. Pyrimidine based heterocycles were investigated with excellent pharmacological activity, however, their photoluminescence activity was never been investigated till now. The presented approach demonstrate a quite novel route for manufacturing of potential military textiles (fluorescent/UV-protective cotton fabrics with micobicide activity) via exploitation of carbon quantum dots (CQDs) nucleated from pyrimidine based heterocycle (*4-(2,4-dichlorophenyl)-6-oxo-2-thioxohexahydropyrimidine-5-carbonitrile*, Target Molecule, TM). The synthesized TM & CQDs were separately immobilized within both of native and cationized cotton fabrics to obtain TM@cotton, CQDs@cotton, TM@Q-cotton and CQDs@Q-cotton fabrics. The estimated yellowness index, intensity of the fluorescence peak, UV-blocking activity and microbicide action, were all followed the order of CQDs@Q-cotton > TM@Q-cotton > CQDs@cotton > TM @cotton. CQDs@Q-cotton showed quite good durability, as after 5 washings, yellowness index was diminished from 26.5 to only 20.3, florescence intensity for CQDs@Q-cotton was decreased from 540 nm to 340 nm and transmission percent was increased from 7 % to 10 %. Moreover, even after 10 washings, microbial inhibition (as a percent) against *E. coli*, *Staphylococcus aureus and Candida albicans* was estimated to 63 %, 68 % and 67 %, respectively, while, UV protection factor (UPF) was diminished from 38.2 (very good) to 21.5 (good). The presented unique route was succeeded for manufacturing of durable fluorescent textiles that could be superiorly applied as potential military textiles.


# Introduction

Military clothes are the first layer to the soldiers for their protection against combat and environmental hazard effects in military missions. Harsh military terrain extensively exerts harmful effects on the physiological and physical performance of some soldiers to cause hazard health problems. Numerous approaches were world widely reported and proceeded within the military/defense researching laboratories in co-operation with industries for manufacturing of technical textiles by incorporation of suitable smart finishing agents for the alleviation of the dangerous effects associated with combat terrains (Perego et al. 2012; Sahin et al. 2005). For manufacturing of military textiles, fabrics must be characterized by, comfortability, easy cared, and easy to be cleaned. Washing durability (Tao et al. 2017) and sterilization or disinfection should be also considered. It could be newly innovative for working towards weaving cotton fabrics with photoluminescence activities, where it acts in transmitting a color to the user's own uniform, identifying the suspected soldier from the same army, while, the absence of a transmitted color would instantly identify enemy.

Numerous reports were considered with acquirement of textiles with additional functions such like color (Emam and Abdelhameed 2017; Ahmed et al. 2018), self-cleaning (Rehan et al. 2013; Emam et al. 2020a; Emam et al. 2018a), luminescent (Emam et al. 2018a), anti-insects (Abdel-Mohdy et al. 2008; Abdelhameed et al. 2017), antimicrobial (Emam et al. 2020b; Ahmed et al. 2017) and UV-protective character (Khan et al. 2015; Nazari et al. 2013; Ates and Unalan 2012; Emam et al. 2020b). Meanwhile,

the development in functionalization of military textiles like tents with enhanced thermal stability, fire resistance, water repellent and anti-insects properties is extremely active topic of research. Additionally for protective masks, air-filtration materials for protection against highly toxic gases, that is, chemical warfare agents, is mainly based on the broad and effective adsorptive properties of functionalizing agents such like, the hydrophobic activated carbons (Li et al. 2011b).

According to literature, few reports were considered with the exploitation of some organic compounds for imparting additional functions for textiles such like triclosan for bactericidal activities, benzophenones for ultraviolet (UV) blocking, dimethylol dihydroxy ethylene urea for acquirement of anti-creasing property, fluorocarbons for hydrophobic capability, long-chain hydrocarbons and polydimethylsiloxanes for textile softening, etc (Almeida 2006; Hewson 1994). Additionally, citric acid, butane tetra-carboxylic acid, and maleic acid (Yang et al. 1998; Welch 1988; Yang et al. 2010) are applied for imparting anti-creasing property to cotton fabric. On the other hand, pyrimidine compounds were differently studied for their successful applicability in various purposes owing to their excellent pharmacological activity (Abuelela et al. 2016). However, according to our knowledge, few researching reports were considered with their application in textile functionalization.

Carbon quantum dots (CQDs) as spherical nanoparticles with particle size of 1–10 nm were ascribed with advantageous characteristics such as high temperature resistance, outstanding electrical /thermal conductivity, high plasticity, corrosion-resistant, UV-blocking, and high adsorption rate as well as catalytic performance (Dasgupta et al. 2016; Kien Nguyen et al. 2016). CQDs as graphite sheets are composed of $sp^2$ carbon atoms formed in planes, while, each carbon atom is mainly bound to three nearest neighbors with 120 degrees apart. The implantation of oxygen, sulfur and nitrogen functional groups that could be introduced on sides of graphite sheet is hypothesized to overcome the inter-sheet van der Waals forces that subsequently resulted in enlargement of the interlayered spacing (Sakthivel and Drillet 2018; Delhaes 2000). Few reports were considered with synthesis of CQDs and their applications in various purposes such as battery, fuel cell, super-capacitor, transistor, biosensor..etc..(Pierson 1993; Wissler 2006; Zhang et al. 2006; Lu et al. 2009). However, according to literature, there is no reports that were investigated the superiority of pyrimidine based heterocyclic compounds as synthesizers for CQDs.

Herein, a new innovative methodology is represented for manufacturing of military textiles. The presented study is concerned with preparation of new fluorescent aromatic compound named as 4-(2,4-dichlorophenyl)-6-oxo-2-thioxohexahydropyrimidine-5-carbonitrile (target molecule, TM) that in turn exploited for synthesis of carbon quantum dots (CQDs). Sequentially, both of TM & CQDs were successively exploited for preparation of durable cotton fabrics as florescent/antimicrobial /UV-protective fabrics, while, the prepared fabrics was evaluated to be functionalized as potential military textile materials. The synthesized TM & CQDs were firstly synthesized and their chemical formulas were affirmed by FT-IR, $^{1}$HNMR and $^{13}$CNMR spectral mapping data. The synthesized TM&CQDs were immobilized within native and cationized cotton fabrics. Afterwards, the modified fabrics were characterized by infrared spectroscopy, scanning electron microscopy, colorimetric measurements, florescence sensitivity, microbicide potency and UV-protective action. The durability of the acquired

fluorescent, antimicrobial and UV-protective characters for modified cotton fabrics was followed up for number of repetitive washings up to 10 cycles.

# Experimental Work

## Materials and chemicals

2,4-Dichlorobenzaldehyde($Cl_2C_6H_3CHO$), Thiourea ($(NH_2)_2CS$) , Ethyl cyanoacetate ($CNCH_2CO_2C_2H_5$), Dimethyl formamide (DMF), Sodium metal and (3-Chloro-2-hydroxypropyl) Trimethyl ammonium chloride (QUAT 188) were purchased from Sigma-Aldrich, assay ≥ 99%. Ethyl alcohol ($C_2H_5OH$), Hydrochloric acid (HCl), Ethyl acetate ($CH_3CO_2C_2H_5$), and *n*-Hexane ($CH_3(CH_2)_4CH_3$) were purchased from Acros Company. All materials were used as supplied without any further purification. Scoured and bleached plain-woven 100% cotton fabrics (185 gm/$m^2$) supported by Misr Company for Spinning and Weaving, El-Mehalla El-Kobra – Egypt.

## Procedure

### *Synthesis of 4-(2,4-dichlorophenyl)-6-oxo-2-thioxohexahydropyrimidine-5-carbonitrile (Target Molecule, TM)*

Mixture of 2,4-dichlorobenzaldehyde (0.01 mol), thiourea (0.01 mol) and ethyl cyanoacetate (0.01 mol) in sodium ethoxide (25 ml; prepared from 1 g sodium metal in 25 ml anhydrous ethyl alcohol) was stirred for 60 minutes at room temperature. Consequently, the reaction mixture was poured in ice bath and neutralized by hydrochloric acid and the precipitated solid was filtered, dried and purified with column chromatography using ethyl acetate: *n*-hexane (2:98) to give reddish yellow crystal with yield percentage of 93% and melting point of 149–151°C.

### *Synthesis of carbon quantum dots (CQDs)*

Carbon quantum dots (CQDs) were synthesized from the synthesized TM via hydrothermal technique as follows; 2 g of TM was dissolved in 100 mL DMF and the liquor was transferred to vertical hydrothermal autoclave reactor and then left in oven at 210 ℃ for 6 hr. The reaction liquor with dark brown color was kept to be cooled at room temperature then dialyzed with DMF by using pur-A-lyzer dialysis kits (MWCO 6-8 kDa from Sigma-Aldrich) for 24 hr to obtain highly purified/monodispersed/pure CQDs, ready for further analyses.

### *Cationization of cotton fabrics*

Cationization of cotton fabric was carried out via interaction with quaternary ammonium salt [(3-Chloro-2-hydroxypropyl) Trimethyl ammonium chloride] in two steps that could be illustrated as follows; in the first step that could be ascribed as activation step, cotton fabric was activated using sodium hydroxide, while, in 250 mL Erlenmeyer flask, 2 g of cotton fabric was soaked in 100 mL of distilled $H_2O$ containing (0.49 g,

12.3 mmol) sodium hydroxide, and then shacked for 2 hr at room temperature. Afterwards, the fabric was removed and washed with distilled $H_2O$ to eliminate excess of sodium hydroxide. The activated fabric was dried in vacuum oven at 60 °C prior to analysis and application.

In the second step that could be identified as cationization step, activated fabric (2 g) was immersed in 50 mL from 60 % of 3-Chloro-2-hydroxypropyl) Trimethyl ammonium chloride. The reaction mixture was shacked in a water bath at 50 ºC for 2 hr. The treated fabric was filtered, washed with distilled water and then dried in vacuum oven at 60 °C and labeled as Q-cotton.

### *Uploading of TM & CQDs onto native and cationized cotton fabrics*

The prepared TM & CQDs were uploaded onto the native and cationized cotton fabrics by dipping methods. 0.25 g the prepared components (TM or CQDs) were dissolved in 25 mL of $CHCl_3$. Pieces of cotton fabrics (0.25 g) were impregnated in the prepared solution for one hour with continuous stirring. Afterwards, fabrics pieces were dried on air before characterization. The obtained fabrics were labeled according to the substituted groups as TM@cotton, CQDs@cotton, TM@Q-cotton and CQDs@Q-cotton.

### Characterization and Instrumental analysis

For Characterization of TM, infrared spectra were recorded on Perkin-Elmer 1600 FTIR (Perkin-Elmer, Waltham, MA, USA) discs. NMR spectra were determined on a Jeol-Ex-300 NMR spectrometer (JEOL, Tokyo, Japan) and chemical shifts were expressed as part per million; (δ values, ppm) against TMS as an internal reference, National Research Center, Cairo, Egypt. $^{1}H$ and $^{13}C$ chemical shifts were referred to the solvent signal (DMSO) at 2.50 and 39.52 ppm, respectively. Data are presented as follows: chemical shift, integration, multiplicity (s = singlet, d = doublet) and coupling constants in Hertz (Hz).

Absorption spectra for TM and the generated CQDs were manifested at 250–750 nm using a spectrophotometer (Cary 100 UV-VIS, UV–Vis-NIR Systems, from Agilent). Topographical structures and size average of the synthesized CQDs were estimated by anticipating of High Resolution Transmission Electron Microscope from Japan (JEOL-JEM-1200). The size average of CQDs were evaluated by 4 pi analysis software (from USA) for 50 particles at least. Infrared spectra was obtained by Jasco FT/IR 6100 spectrometer, while, the absorbance spectral data were detected at 500 – 4000 $cm^{-1}$ using 15 points smoothing, 4 $cm^{-1}$ resolution, 64 scanning times with scanning rate of 2 $mm.sec^{-1}$. The spectral mapping data of nuclear magnetic resonance ($^{1}H$-NMR and $^{13}C$-NMR) were obtained by Jeol-Ex-300 NMR spectrometer (JEOL – Japan). Photoluminescence for the prepared CQDs in ultraviolet-visible range were followed up by spectro-fluorometer (JASCO FP8300). The data were estimated at room temperature with excitation at 340 nm.

Material contents in terms of nitrogen content (N%) of the TM & CQDs applied onto cotton fabrics before and after washing cycles were evaluated were measrured according to Kjeldahl method (Emam et al. 2018b). Mixture (a) was preliminary prepared by mixing in powder form of (10 g) $CuSO_4$, (90 g) $K_2SO_4$ and (1 g) selenium. Indicator was prepared by dissolving both of methyl red (0.125 g) and methylene blue

(0.083 g) separately in 50 mL absolute alcohol and subsequently mixed together with equal volumes. Afterwards, solution (b) was prepared by addition of the indicator to 4% boric acid (25 mL). In brief, specific weight of the samples (100 – 150 mg) were digested completely with 1 g of mixture (a) in 10 mL of sulfuric acid via mental heater until cololrelss solution is obtained. Flask content was trasnfered carefully to the Kjeldahl apparatus and then sodium hydroxide solution (0.1 N) was added till violet color was observed. The vapour was received in flask containing solution (b) and then titrated with hydrochloric acid (0.05 N) until the color was changed to violet color. The contents of nitrogen were evaluated as percentage by identifying the titrated volume, then the concentration of HCl and normalized to the weight of sample.

The treated fabrics were investigated under high resolution scanning electron microscope (HRSEM Quanta FEG 250 with field emission gun, FEI Company – Netherlands). The elemental analysis was also estimated from the energy dispersive X-ray analyzer (EDAX AME-TEK analyzer). The infrared spectra for the modified fabrics (CQDs@cotton and CQDs@Q-cotton) were measured by using Jasco FT/IR 6100 spectrometer. The absorbance spectra were ranged in 4000 – 400 $cm^{-1}$ using 4 $cm^{-1}$ resolution and 64 scanning times with rate of 2 mm/sec.

The colorimetric data (L, a*, b*, absorbance, color strength [K/S] and yellowness index [YI E313]) were all estimated for the modified fabrics using spectrophotometer attached with pulsed xenon lamp (UltraScan Pro, Hunter Lab, USA), while, color coordinates parameters of L*, a* and b* that are referring to the lightness (black/white, 0/100), the red/green ratio (+/-) and the yellow/blue ratio (+/-), respectively (Ahmed et al. 2017; Ahmed et al. 2018). The measurements were performed three times at different measurements areas in order to estimate the average values.

### *Optical properties*

The digital photos for TM and CQDs were carefully captured inside the box of UV lamp (output 4 W and input 220 V AC). Photos of samples were taken upon excitation at 325 nm by cell phone camera of Oppo A31 model.

The absorbance spectra for TM and CQDs were measured using FLAME-S-UV-VIS spectrometer from USA. Fluorescence were also monitored by Jasco FP-6500 spectro-fluorometer (150 W Xenon lamp, with concave holographic grating (1800 grooves/mm emission monochromator and coupled with a second photomultiplier) from Japan. The samples were excited at wavelength of 360 nm and the emission spectra were then detected at room temperature.

### *Transmission and Ultraviolet Radiation Blocking*

Ultra-violet radiation (UVR) transmission spectral results (T %) over native and cationized cotton before and after successive uploading of the prepared TM&CQDs were measured by using JASCO V-750 spectrophotometer from Japan in range of 280–400 nm with 2 nm interval. In addition to, UV protection factor (UPF), blocking in UV-A (315–400) region (UVA) and blocking in UV–B (280–315) region (UVB) were

all estimated using AATCC Test Method 183–2010.44. For each sample, the measurement were carried out for two times in different areas, and the average was evaluated.

### *Microbicide potentiality*

The antimicrobial potentiality of TM, CQDs and the modified fabrics against different pathogenic species was approved via the qualitative method of a Kirby-Bauer disk diffusion technique (Bayer et al. 1966; Ahmed et al. 2019). In this procedure, all of the prepared TM, CQDs and the modified fabrics were examined for antimicrobial performance against three different pathogenic species of Gram-positive bacteria: *Staphylococcus aureus* (*NCTC-7447*), Gram-negative bacteria: *Escherichia coli* (*NCTC-10416*) and unicellular fungi: namely, *Candida albicans(NCCLS 11)*. To estimate the lowest concentration of the prepared TM and CQDs that showed an observable inhibition in microbial growth, the minimal inhibitory concentration (MIC) was estimated. MIC was calculated for the crude antimicrobial material according to (El-Naggar et al. 2020b) using serial dilution method via turbid metric technique according to the procedure described in literature (El-Naggar et al. 2020a; Hasanin and Moustafa 2020; Salama et al. 2020). The antimicrobial test of samples was carried out using 0.5 g following the cell formation unit counting (CFU) technique as described in literature (El-Naggar et al. 2020a; Hasanin and Moustafa 2020; Salama et al. 2020).

Additionally, the disk diffusion test (inhibition zone technique) was also performed for evaluation of the microbicide effeceincy of the prepared samples. The different tested bacterial strains were grown in the media for preparation of pathogenic suspension.100 µL of bacterial suspension was spreaded onto agar plates corresponding to the broth in which it was maintained. A 10 µL of the tested compounds was placed on the middle of plates and then incubated at 37 °C for 24h. The diameters of the inhibition zones were evaluated in millimeters using slipping calipers according to NCCLS, 1997 (CLSI 2012). In MIC determination, serial dilutions from the tested solutions (0–1000 µL/mL) were prepared and then added to the plates. After incubation at 37 °C for 24 h, the colony forming units (CFU) were counted for each dilution (Emam et al. 2017; CLSI 2012).

### *Washing durability*

Washing durability of the modified fabrics was monitored via the repetitive washing cycles up to five cycles. Washing was carried out according to the AATCC standard method for the home laundry test (AATCC 2010). Washing procedure was performed by using a mixture of 2 g/L of sodium carbonate and 1 g/L of commercial detergent as washing solution. The modified fabrics were immersed in washing solution at 60 ± 3 °C using 1:100 material to liquor ration under continuous stirring. After 15 minutes, the fabrics were removed from washing liquor, gently squeezed, rinsed with tap water and then dried at 70 ± 3 °C prior to further instrumental characterizations. The washing process was furtherly repeated for five times to get the required five washing cycles.

## Results And Discussion

### *Synthesis of TM*

The reaction mechanism for synthesis of TM could be briefly illustrated as in the presence of sodium ethoxide, active carbanion is supposed to be produced within reaction mixture from ethyl cyanoacetate (Figure 1). Afterwards, nucleophilic addition reaction on carbonyl group of 2,4-dichlorobenzaldehyde with the produced carbanion was subsequently proceeded to give the first synthetic equivalent (**1**). Lastly, interaction between thiourea and synthetic equivalent **(1)** resulted in cyclization with elimination of water and ethanol to produce the desirable TM **(2)**.

The structural formula of the prepared TM was confirmed via different spectral mapping data (IR, $^{1}$HNMR and $^{13}$CNMR) and the data were presented in Figure 2. The represented data showed that, IR spectrum (KBr, v, $cm^{-1}$) for TM was especially characterized with number of peaks at 3377-3248, 3127, 2671 2171 and 1609, 1467 &1409, 1086 and 730-630 $cm^{-1}$ corresponding to (2NH), (=CH), (-CH), (CN), (C=O), (C-C aromatic), (C=S) and (C-Cl) respectively. $^{1}$H NMR spectral data (300 MHz, DMSO-$d_6$, δ ppm) was represented with number of characteristic peaks that could be interpreted as follows; 5.14 (d, *J*=12.4 Hz, 1H, CH-CN), 5.70 (d, *J*=12.4 Hz, 1H, CH), 7.61 (d, *J* = 1.8 Hz, 1H, Ar-H), 7.66 (s, 1H, Ar-H), 7.71 (d, *J* = 1.9 Hz, 1H, Ar-H), 7.71 (d, *J* = 1.9 Hz, 1H, Ar-H), 10.11 (s, 1H, NH; $D_2O$ exchangeable), 11.81 (s, 1H, NH; $D_2O$ exchangeable). On the other hand, $^{13}$C NMR (75 MHz, DMSO, δ ppm) spectral mapping data were given further confirmable overview for the chemical formula of the synthesized TM and represented a number of detected bands at 50.53 ($SP^3$-C, C-CN), 52.20 ($SP^3$-C), 114.13 (CN), 128.29 (Ar-C), 129.34 (Ar-C), 131.05 (Ar-C), 132.06 (Ar-C), 134.52 (Ar-C), 134.82 (Ar-C), 159.89 (C=O) and 178.78 (C=S).

### *Synthesis of CQDs*

Clustering of CQDs was successively performed via hydrothermal technique from the synthesized TM (Figure 1). According to literature, the mechanism for synthesis of CQDs could be postulated as follows: the prepared TM is supposed to be hydrolyzed and fragmented under the hydrothermal conditions. Consequently, polymerization, aromatization and afterwards oxidation were proceeded to give aromatic graphite sheets decorated with nitrogen, sulfur and nitrogen containing functional groups, for generation of size and shape regulatable CQDs (Li et al. 2011a; Sakaki et al. 1996; Chen et al. 2013).

### *Characterization of CQDs*

UV-Visible spectral data for both of TM and CQDs were plotted in Figure 3a. From the visual observation of TM and CQDs solutions, the yellowish color of TM was turned to darker yellow after the hydrothermal conditions for clustering of CQDs. The plotted absorbance spectra for the synthesized TM & CQDs showed a characteristic absorption peak at 440 nm for n-π* (C=X) (Kim et al. 2018; Kim et al. 2019; Luo et al. 2009; Wu et al. 2014). However, there was significant decreasing in intense for the detected band with ingraining of CQDs, that was in agreement with literature (Gao et al. 2016), while, the optical absorption

spectra of CQDs was mainly detected with lower intense, attributing to decomposition of TM and subsequent polymerization for generation of CQDs (Chae et al. 2017; Pires et al. 2015; Zuo et al. 2015; Chandra et al. 2012; Gao et al. 2017; Liu et al. 2016; Song et al. 2018).

The topographical features and geometrical shape of TM and CQDs were presented in the micrographs of Transmission Electron Microscope (TEM) from which their size distribution was estimated and plotted. The micrographs showed that, the synthesized CQDs were homogenously/well dispersed and controllably clustered in the reaction medium with quite smaller size rather than TM. TM detected with mean size of 544.6 nm, while, CQDs exhibited quite smaller mean size of 6.5 nm. This could be explained as, under strong alkaline conditions, the hydrothermal technique successively resulted in fragmentation of TM, polymerization and aromatization of the liberated fragments to generate controllably sized CQDs. These could approve the compatibility of the synthesized TM in generation of CQDs under hydrothermal conditions (Figure 3 b & c).

Figure 4a represented FT-IR spectrum for CQDs prepared from the synthesized TM, to show that, six characteristic peaks of CQDs at 3161 $cm^{-1}$ (=CH, stretching), 2924 $cm^{-1}$ (CH, stretching), 2055 $cm^{-1}$ (C=O, conjugated acid halide), 1632 $cm^{-1}$ (C=O, amide), 1531-1406 $cm^{-1}$ (C=C aromatic), 1142 (C-O-C, stretching). On the other hand, NMR spectral mapping data were presented in figure 4b&c for CQDs. $^{1}$HNMR for CQDs prepared from TM (Fig.4b) showed the existence of characteristic peaks of protons on carbon next to aryl group at 2.48 ppm, protons for on a carbon attached to oxygen at 2.87 ppm, aromatic or $sp^2$ CH=CH protons & CO-$NH_2$ protons at 6.71-7.40 ppm and protons of hydroxyl decorative groups at 8.11 ppm protons.

Figure 4c represented $^{13}$CNMR spectra of the prepared CQDs and it could be obviously showed that, the typical bands for CQDs at 30.86 ppm, 99.89 ppm, 131.82 ppm, and 175.96 ppm & 183.96 ppm, which were corresponding to $sp^3$ carbons, carbons of C-O, carbons in aromatic rings, C=C aromatic or $sp^2$ carbons and carbons of C-OH & C-SH groups, respectively, were detected.

### *Modification of fabrics with TM & CQDs*

The synthesized TM & CQDs were applied onto the cotton and cationized cotton fabrics. The prepared TM could be chemically interacted with the cotton fabrics via hydrogen bonding through the hydroxyl groups of cellulosic backbone of cotton and the functional or decorative groups (OH, NH, $NH_2$, O, N, S) of TM or CQDs (Emam et al. 2018b; Abdelhameed et al. 2018; Emam et al. 2020a) (Figure 5). For cationized cotton, in addition to hydrogen bonding, dipole-dipole interaction is supposed to be existed between the fabric backbone and the functional or decorative groups of TM or CQDs. Besides, TM or CQDs might be physically entrapped within the intermolecular pores and spaces of fabric matrix (Abdelhameed et al. 2018; Emam et al. 2020b).

### *SEM & EDX*

The morphological features for the surface of the treated native and cationized cotton fabrics were investigated and plotted in Figure 6. For native cotton, cationized cotton, TM@cotton, CQDs@cotton, TM@Q-cotton and CQDs@Q-cotton, SEM images, EDX signals and elemental analysis were presented. Before treatment with the prepared TM & CQDs, the surface of fabrics was seemed to be smooth, and the characteristic peaks of C & O were only detected native in case of native cotton, while, cationized fabric was characterized with C, O & N bands (Fig.6 a & b). After modification, the particles of TM & CQDs were observably distributed on the surface of cotton. For all the modified fabrics, EDX analysis showed the four characteristic signals of C, O, N, S & Cl elements, which affirmed the immobilization of the applied TM & CQDs onto the treated fabrics. However, dense masses of the prepared TM & CQDs were observed in case of cationized fabrics rather than the native ones, attributing to the higher accessibility of fabrics with cationization. Moreover, CQDs@Q-cotton were observed with more dense masses on the surface rather than TM@Q-cotton, due to the higher opportunities of entrapping more amounts of smaller sized CQDs rather than TM, that in-turn affirmed the above-postulated mechanism.

### *FTIR*

The unmodified and modified cotton fabrics were characterized by FTIR as presented in Figure 7. The plotted spectral data showed that, both of native and cationized cotton fabrics exhibited characteristic absorption bands of O-H (3330 – 3289 $cm^{-1}$), C-H aliphatic (2888 $cm^{-1}$), weak band for C=O (1634 $cm^{-1}$), H-C-H (1417 $cm^{-1}$), asymmetric C-O-C (1150 $cm^{-1}$), and C-C (1072 $cm^{-1}$) (Emam and Abdelhameed 2017; Emam and Bechtold 2015). However, after modification with the synthesized TM and CQDs, all of the referred absorbance bands were retained, in addition to new bands for S-H (2600 $cm^{-1}$) and aliphatic C-S (630-790 $cm^{-1}$). Whereas, the characteristic bands of C=O, H-C-H & asymmetric C-O-C became more intense, confirming the successive chemical bonding and immobilization of the prepared TM & CQDs within cotton matrix.

### *Material contents & Color data*

Table 1 represented the nitrogen contents estimated for TM & CQDs, in addition to native and cationized fabrics before and after uploading of the prepared TM & CQDs. Moreover, the effect of washing on the estimated values of material contents was followed up for all the treated sample. The data showed that, material contents was significantly higher in case of cationized fabrics rather than native ones, in addition to, fabrics treated with CQDs exhibited higher material contents rather than that treated with TM. From the evaluated data, CQDs@Q-cotton showed the highest material content percent of 7.56 %, while, after ten repetitive washings, the material content percent was diminished to 4.92 %, to give more affirmation for higher accessibility of fabrics with cationization in more efficient preservation of the uploaded CQDs.

**Table 1:** Material contents onto the functionalized cotton fabrics before and after washing.

| Fabric | N Content (%) | N Uploading (%) | Material content (%) |
|---|---|---|---|
| **TM** | 19.78 | – | – |
| **CQDs** | 19.32 | – | – |
| **Cotton** | 0.00 | 0.00 | 0.00 |
| **TM@Cotton** | 0.87 | 0.87 | 4.39 |
| **CQDs@Cotton** | 1.08 | 1.08 | 5.59 |
| **Q-Cotton** | 0.51 | 0.00 | 0.00 |
| **TM@Q-Cotton** | 1.78 | 1.27 | 6.42 |
| **CQDs@Q-Cotton** | 1.97 | 1.46 | 7.56 |
| **5-W-Q-Cotton** | 0.43 | 0.00 | 0.00 |
| **5W-TM@Q-Cotton** | 1.55 | 1.04 | 5.26 |
| **5W-CQDs@Q-Cotton** | 1.78 | 1.27 | 6.57 |
| **10-W-Q-Cotton** | 0.21 | 0.00 | 0.00 |
| **10W-TM@Q-Cotton** | 1.24 | 0.73 | 3.69 |
| **10W-CQDs@Q-Cotton** | 1.46 | 0.95 | 4.92 |

The color data for the modified fabrics were presented in Table 2 & Figure S1 in supplementary file. From the estimated data, the cotton fabrics were acquired yellowish color after modification owing to the yellow color of TM. YI (yellowness index) was extremely higher in case cationized cotton compared cotton fabrics. In addition to, fabrics modified with CQDs exhibited higher yellowness degree rather than that modified with TM. The modification of cationized cotton fabric with CQDs showed the highest yellowness index and lowest whiteness index. The strength of yellow color was ordered as follows; CQDs@Q-cotton > TM@Q-cotton > Q-cotton > CQDs@cotton > TM@cotton > cotton. Table S1 in supplementary file revealed that, after five repetitive washing cycles, the estimated values of YI for all the tested samples were insignificantly decreased. YI was detected to be 26.5 for CQDs@Q-cotton, while, after 5 washing cycles it was diminished to be 20.3.

**Table 2:** Colorimetric data for the functionalized cotton fabrics before and after washing.

| Fabric | L* | a* | b* | WI E313 [D65/10] | YI E313 [D65/10] | Absorbance (370 nm) | K/S (370 nm) |
|---|---|---|---|---|---|---|---|
| **Cotton** | 83.9 | -0.1 | 0.2- | 58.9 | 0.4 | 0.3 | 0.2 |
| **TM@Cotton** | 82.3 | -0.5 | 1.5 | 53.1 | 2.9 | 0.4 | 0.5 |
| **CQDs@Cotton** | 82.3 | -0.8 | 2.1 | 50.2 | 3.8 | 0.5 | 0.6 |
| **Q-Cotton** | 82.6 | 0.4 | 10.4 | 8.5 | 21.6 | 0.5 | 0.8 |
| **TM@Q-Cotton** | 81.8 | 0.4 | 12.9 | 6.3 | 26.5 | 0.6 | 1.2 |
| **CQDs@Q-Cotton** | 82.1 | -1.0 | 11.3 | 4.9 | 21.9 | 0.7 | 1.4 |
| **5W-TM@Cotton** | 82.1 | -0.3 | 1.3 | 51.8 | 2.4 | 0.3 | 0.4 |
| **5W-CQDs@Cotton** | 82.4 | -0.6 | 1.8 | 49.7 | 2.9 | 0.3 | 0.3 |
| **5W-Q-Cotton** | 82.6 | 0.4 | 10.4 | 8.5 | 21.6 | 0.5 | 0.8 |
| **5W-TM@Q-Cotton** | 82.1 | 0.1 | 11.1 | 11.3 | 20.3 | 0.5 | 0.8 |
| **5W-CQDs@Q-Cotton** | 82.2 | -0.4 | 10.8 | 9.9 | 17.0 | 0.5 | 1.0 |

### *Optical and Fluorescence properties*

Principally, the absorption spectra of TM and CQDs are related to their fluorescence sensitivity, that might attributed to their inter-construction with heteroatoms of (N, S, O & Cl) and decoration with substituted groups (OH, $NH_2$, S & Cl) (Wu et al. 2014; Gao et al. 2016). Hence, the optical properties of the prepared TM & CQDs are owing to the overlapping of π-π* and n-π* transitions with the decorative functional groups.

The fluorescence spectra for both of TM & CQDs were measured after excitation at 440 nm as shown in Figure 8a. The excited TM showed a fluorescence peak lesser than 200 nm, which is related to the green area as mentioned in literature (Shao et al. 2016; Li et al. 2017). The excited CQDs uniquely showed with greatly higher intensed peak at more than 1000 nm, that could be attributed to extensive higher aromatic character of CQDs with their decorative substituents which extensively shared in extension of conjugation resulted significantly observable jumping in their fluorescence intentsity. Figure 8b, represented the fluorescence intensity for cotton and cationized cotton after modification with both of TM & CQDs. The spectral data affirmed that, fluorescence intensity was corresponding to the following order; CQDs@Q-cotton > CQDs@cotton > TM@Q-cotton > TM @cotton. Meanwhile, cationization of cotton fabrics resulted in higher affinity for successive impregnation of CQDs in greater quantities within cotton matrix, leading to CQDs@Q-cotton extinesively exhibit the highest fluorescence intensity (560 nm) corresponding to yellow emission.

In textile industrialization, washing durability is highly demanded to be acquired and hence it must be well-considered in the current approach. The fluorescence spectra were measured for the modified cotton fabrics after 5 and 10 washing cycles, while the data were shown in Figure 8c & d. The fluorescence spectra similar to that of the unwashed fabrics, while, the fluorescence intensity was observably decreased with washing due to leaching out the applied fluorescent active TM & CQDs. Increment in the number of washing cycles logically resulted in further diminishing in the fluorescence intensity of the modified fabrics. However, even after 10 washing cycles the modified fabrics still exhibited fluorescent character with good washing fastness with sequential laundry.

Photoluminescent textile are commonly reported to be prepared by immobilization of metallic compounds such as nanoparticles (Zhang et al. 2015), metal organic framework (Emam et al. 2018a) and materials doped with metal salts ($Zn^{+2}$ & ZnS) (Du et al. 2018; Zhang et al. 2017a; Zhang et al. 2017b). referring to the as-mentioned reports, the prepared fluorescent modified cotton fabrics in the current work could be ascribed to be more durable than the textiles treated with AuNPs and Ln ($Eu^{+3}$ & $Tb^{+3}$)-metal organic frameworks (Emam et al. 2018a). The fluorescence intensities of the modified cotton fabrics were observably higher than that estimated for Au nanoparticles@silk, $Zn^{+2}$ doped carboxymethyl cellulose, ZnS containing hydrogel@spandex and fluorene containing polymers@cellulose (Zhang et al. 2015; Du et al. 2018; Zhang et al. 2017a; Zhang et al. 2017b; Phung Hai and Sugimoto 2017). These findings could declare that, the synthesized TM & CQDs could promisingly applied for manufacturing of highly actively fluorescent textiles with substantial washing fastness rather than that previously reported in literature which were interested in preparation of photoluminescent textiles.

### *UV-protection*

Transmission percent (T %) as a key factor for monitoring the ultraviolet blocking capability for all tested specimens was estimated and plotted in Figure 9. It could be clearly observed that, T% was greatly diminished for all the tested fabrics by modification with both of TM & CQDs compared to the untreated specimens. Unmodified cotton fabric showed the highest transmission percent (60 % at 400 nm). Diminishing in T% was much higher in cationized cotton, owing to its inter-composition with greater amounts of TM & CQDs. The results showed that, T% was decreased from 15% for cationized cotton to 6% and 5% for TM@Q-cotton and CQDs@Q-cotton, respectively. After 5 washing cycles, T% was insignificantly increased to 40% for CQDs@cotton. With cationization of fabric, the uploaded CQDs were more retained against washings, as T% was increased un-sensibly up to 10% for CQDs@Q-cotton. So it could be depicted that, cationization is superiorly affected in more stably and stronger interaction of CQDs with fabric building blocks.

**Table 3:** Data of transmission and UV-protection through the functionalized cotton fabrics before and after washing.

| Fabric | (T%) UVA | (T%) UVB | UVA Blocking | UVB Blocking | UPF | Rating |
|---|---|---|---|---|---|---|
| **Cotton** | 66.0 | 83.3 | 34.0 | 16.7 | 1.3 | Insufficient |
| **TM@Cotton** | 35.0 | 22.3 | 75.0 | 77.7 | 5.2 | Insufficient |
| **CQDs@Cotton** | 26.7 | 18.5 | 73.3 | 81.5 | 5.5 | Insufficient |
| **Q-Cotton** | 15.3 | 11.6 | 84.7 | 88.4 | 8.1 | Insufficient |
| **TM@Q-Cotton** | 6.5 | 3.9 | 93.5 | 96.1 | 29.4 | Very Good |
| **CQDs@Q-Cotton** | 5.2 | 3.0 | 94.8 | 97.0 | 38.2 | Very good |
| **5W-TM@Cotton** | 50.7 | 49.6 | 49.3 | 50.4 | 4.1 | Insufficient |
| **5W-CQDs@Cotton** | 37.9 | 26.7 | 62.1 | 73.3 | 3.1 | Insufficient |
| **5W-TM@Q-Cotton** | 9.5 | 7.2 | 90.5 | 92.8 | 18.2 | Insufficient |
| **5W-CQDs@Q-Cotton** | 5.6 | 3.2 | 94.6 | 96.9 | 32.6 | Very Good |
| **10W-TM@Q-Cotton** | 15.3 | 10.6 | 84.7 | 89.4 | 11.9 | Insufficient |
| **10W-CQDs@Q-Cotton** | 10.3 | 5.6 | 89.7 | 94.4 | 21.5 | Good |

UV protection character for fabrics was relied on three key factors, firstly the fabric structure in addition to the type of the compound with which they were modified, i.e. either TM or CQDs with their topographical features. For all tested fabrics, UV protection in B-region was relevantly lower than that in A-region. Ultraviolet protection factor (UPF) was detected from T% results (Table 3), and it was 1.3 and 8.1 for native cotton and cationized cotton fabrics, whereas it was estimated to increase up to 5.2, 5.5, 29.4 and 38.2 for TM@cotton, CQDs@cotton, TM@Q-cotton and CQDs@Q-cotton, respectively. Referring to materials contents (Table 1), the highest UPF value was estimated for CQDs@Q-cotton to affirm the prior cationization effect in more efficient uploading and higher amounts of CQDs within fabric matrix. In addition to approving the higher compatibility of CQDs for reflecting more radiation rather than TM. Moreover, after washing, UPF values were diminished for the cationized fabrics after ten cycles, as it was lowered from 38.2 to 21.5 for CQDs@Q-cotton that reflected the washing durability of the prepared samples, to give more confirmation for the effect of cationization in stronger and more efficient immobilization of CQDs within fabric polymeric blocks.

From the above-illustrated results it could be mentioned that, comparing with other reports for preparation of UV-protective cotton via direct deposition of metals on cotton fabrics, UV protection properties for CQDs@Q-cotton was considerably higher, regardless to the metal type (Ag, Au, Zn, Cu or Ti) (Emam and Bechtold 2015; Ahmed et al. 2017; Emam et al. 2016). Moreover, similar UV protection results were obtained for MOF@textiles (Emam and Abdelhameed 2017; Emam et al. 2020b). This comparison

approved the higher efficiency of the presented methodology for functionalization of cotton fabric to be UV protective fabrics.

### *Microbicide potentiality*

According to literature (Li et al. 2018; Li et al. 2016; Ipe et al. 2005; Dong et al. 2020; Ristic et al. 2014; Stanković et al. 2018; Kováčová et al. 2018), the mechanism of antimicrobial performance for the as-synthesized CQDs could be illustrated as follows; under the visible light in aqueous medium, CQDs are capable of eliminating reactive species (RS), such as singlet oxygen and hydroxyl free radicals that are mainly responsible for microbial cell mortality. The reactive species (RS) were suggested to adhere then penetrate the microbial cell wall for motivation of the oxidative stress and fragmentation of DNA & RNA, resulting in inhibition and corruption of the gene expression. In addition to, RS could play a main role in the mitochondrial dysfunction, inactivation of intracellular protein, lipid peroxidation, gradual damaging of the cell wall, followed by necrosis / apoptosis and microbial cell mortality.

In the represented approach, the microbicide potentiality for the synthesized TM & CQDs with different concentrations was estimated against three different pathogenic species of positive gram bacteria (*S. aereus*), negative gram bacteria (*E. coli*) and fungal species (*C. albicans*) via inhibition zone technique with evaluation of the minimal inhibitory concentration (MIC) of the synthesized TM & CQDs. The estimated data in Table 4 significantly revealed that, against all the tested bacterial and fungal species, CQDs (100 mg/ml) showed the highest antimicrobial potency with microbial inhibition percentage (MIC%) reached 100 % against all the tested species, while, the same concentration of TM showed significant lowered MIC percentage of 89.0 ± 1.2 %, 92.0 ± 1.1 % and 77.0 ± 1.5 % against *E. coli, S. aereus & C. albicans,* respectively. The excellence microbicide potency of CQDs is mainly attributed to its highly size and shape regulation and organization, to be easily penetrated through the microbial cell membrane, leading to eventual cell mortality. The estimated results are in accordance with literature (Li et al. 2018; Dong et al. 2020; Ristic et al. 2014; Stanković et al. 2018; Kováčová et al. 2020) while, the excellence of the synthesized CQDs as potential antimicrobial laborers are mainly attributed to their inter-construction of decorative functional groups that mainly acted in the microbial cell death via production of RS.

**Table 4:** The results of MIC (inhibition %) for the prepared carbon quantum dots compared to the target molecule.

| Material | Conc. (mg/mL) | *E. coli* | *Staphylococcus aureus NCTC-7447* | *Candida albicans NCCLS 11* |
|---|---|---|---|---|
| **TM** | 100.0 | 89.0 ± 1.2 | 92.0 ± 1.1 | 77.0 ± 1.5 |
| | 50.0 | 47.0 ± 1.1 | 51.0 ± 1.5 | 32.0 ± 1.5 |
| | 25.0 | 17.0 ± 1.2 | 32.0 ± 1.2 | 21.0 ± 0.9 |
| | 12.5 | 0.0 | 14.0 ± 0.7 | 15.0 ±0.7 |
| | 6.25 | 0.0 | 0.0 | 0.0 |
| | 3.125 | 0.0 | 0.0 | 0.0 |
| **CQDs** | 100.0 | 100.0 | 100 | 100 |
| | 50.0 | 100 | 100 | 77.0 ± 1.1 |
| | 25.0 | 59.0 ± 1.0 | 78.0 ± 1.2 | 53 ± 0.8 |
| | 12.5 | 31.0 ± 0.9 | 45.0 ± 1.0 | 27.0 ± 0.8 |
| | 6.25 | 22.0 ± 0.7 | 23.0 ± 0.9 | 16.0 ± 0.5 |
| | 3.125 | 18.0 ± 0.6 | 11.0 ± 0.5 | 9.0 ± 0.3 |
| | 1.562 | 9.0 ± 0.3 | 0.0 | 0.0 |

Table 5 represented the antimicrobial potentiality of the unmodified and modified fabrics, before and after 5 & 10 washing cycles. From the evaluated results, it could be depicted that, the synthesized TM & CQDs showed to acquire the cotton fabrics superior antimicrobial activity. CQDs@Q-cotton showed to exhibit the highest antimicrobial performance, with inhibition percentage of 71.0 ± 1.1 %, 82.0 ± 1.0 % and 62.0 ± 0.9 % against *E. coli, S. aureus and C. albicans*, respectively, relating to the effect of cotton cationization in increment of the immobilization affinity for CQDs, CQDs@Q-cotton. Moreover, by monitoring the washing durability of the modified fabrics for their antimicrobial performance, the tabulated data revealed that, even after 10 washing cycles, CQDs@Q-cotton fabric still exhibited good microbicide potency, whereas, microbial inhibition percent was evaluated to be 55.0 ± 0.9%, 61.0 ± 1.1% and 32.0 ± 0.6% against the tested microbes.

**Table 5:** Biological activities results (inhibition %, CFU) for the functionalized cotton fabrics before and after washing.

| Samples | *E. coli* | *Staphylococcus aureus NCTC-7447* | *Candida albicans NCCLS 11* |
|---|---|---|---|
| **TM** | 89.0 ± 1.2 | 92.0 ± 1.1 | 77.0 ± 1.5 |
| **CQDs** | 100.0 | 100.0 | 100.0 |
| **Cotton** | 0.0 | 0.0 | 0.0 |
| **TM@Cotton** | 39.0 ± 1.4 | 44.0 ± 1.1 | 49.0 ± 1.1 |
| **CQDs@Cotton** | 63.0 ±0.9 | 68.0 ± 1.9 | 67.0 ± 1.8 |
| **Q-Cotton** | 16.2 ± 0.5 | 21.1 ± 0.9 | 19.6 ± 1.0 |
| **TM@Q-Cotton** | 55.0 ± 1.9 | 59.0 ± 1.2 | 62.0 ± 1.7 |
| **CQDs@Q-Cotton** | 78.0 ± 1.1 | 77.0 ± 1.3 | 81.0 ± 1.4 |
| **5W-TM@Cotton** | 15.7 ± 0.6 | 19.9 ± 0.8 | 21.2 ± 1.1 |
| **5W-CQDs@Cotton** | 42.0 ± 0.6 | 59.0 ± 1.2 | 62.0 ± 1.7 |
| **5W-TM@Q-Cotton** | 46.0 ± 1.8 | 59.0 ± 1.5 | 52.0 ± 1.4 |
| **5W-CQDs@Q-Cotton** | 71.0 ± 1.1 | 82.0 ± 1.0 | 78.0 ± 1.6 |
| **10W-TM@Q-Cotton** | 41.0 ± 1.4 | 45.0 ± 1.7 | 49.0 ± 0.9 |
| **10W-CQDs@Q-Cotton** | 63.0 ± 0.9 | 68.0 ± 1.9 | 67.0 ± 1.8 |

# Conclusion

In the current approach, fluorescent *4-(2,4-dichlorophenyl)-6-oxo-2-thioxohexahydropyrimidine-5-carbonitrile (Target Molecule, TM)* was newly synthesized and exploited in nucleation of carbon quantum dots (CQDs). The strucutral formulas for both TM & CQDs were affirmed by IR and NMR spectral analyses. The synthesized TM & CQDs were uploaded onto native and cationized cotton fabrics and the modified fabrics were characterized by yellowish color. Under UV lamp at 325 nm, all of the modified fabrics were exhibited green emission. After excitation at 440 nm, the modified cationized fabrics were showed an intense emission peak at 540 nm by modification with CQDs. The yellowness degree,

fluorescence intensity, UV-protection and microbicide actions were followed the order of CQDs@Q-cotton > TM@Q-cotton > CQDs@cotton > TM@cotton. Durability for all prepared samples were monitored for the washing for 10 repetitive washing cycles, while CQDs@Q-cotton showed to superior retaining for the acquired florescent sensitivity, UV-protection and antimicrobial actions with good durability which was explained by the effect of cotton cationization in stronger and stably immobilization of the applied CQDs within fabric matrix.

The current work opened unique/novel challenge in the textile industry to obtain durable photoluminescent/UV-protective textiles with excellent microbicide activity by using the prepared CQDs. Moreover, the synthesized CQDs could also be promising for several purposes such as smart labeling, anti-counterfeiting, sensors/biosensors, bio-imaging and tissue engineering.

# Declarations

**Compliance with ethical standards:** ***The authors declare that they have no competing financial interest***

**Conflict of interest:** ***There is no conflict of interest***

**Ethical approval:** ***Not applicable***

# References


1. AATCC (2010) Standardization of Home Laundry Test Conditions. AATCC Technical Manual 85:401
2. Abdel-Mohdy F, Fouda MM, Rehan M, Aly A (2008) Repellency of controlled-release treated cotton fabrics based on cypermethrin and prallethrin. Carbohydrate polymers 73(1):92–97
3. Abdelhameed RM, El-Zawahry M, Emam HE (2018) Efficient removal of organophosphorus pesticides from wastewater using polyethylenimine-modified fabrics. Polymer 155:225–234
4. Abdelhameed RM, Kamel OM, Amr A, Rocha Jo, Silva AM (2017) Antimosquito activity of a titanium–organic framework supported on fabrics. ACS Appl Mater Interfaces 9(27):22112–22120
5. Abuelela AM, Mohamed TA, Wilson LD, Zoghaib WM (2016) Raman and infrared spectra, normal coordinate analysis and ab initio calculations of 4-Amino-2-chloropyrimidine-5-carbonitrile. J Mol Struct 1115:85–93
6. Ahmed HB, Attia MA, El-Dars FM, Emam HE (2019) Hydroxyethyl cellulose for spontaneous synthesis of antipathogenic nanostructures:(Ag & Au) nanoparticles versus Ag-Au nano-alloy. Int J Biol Macromol 128:214–229
7. Ahmed HB, El-Hawary NS, Emam HE (2017) Self-assembled AuNPs for ingrain pigmentation of silk fabrics with antibacterial potency. Int J Biol Macromol 105:720–729
8. Ahmed HB, Emam HE, Mashaly HM, Rehan M (2018) Nanosilver leverage on reactive dyeing of cellulose fibers: color shading, color fastness and biocidal potentials. Carbohydrate polymers 186:310–320

9. Almeida Ld (2006) Functionalisation of textiles: future perspectives
10. Ates ES, Unalan HE (2012) Zinc oxide nanowire enhanced multifunctional coatings for cotton fabrics. Thin Solid Films 520(14):4658–4661
11. Bayer A, Kirby W, Sherris J, Turck M (1966) Antibiotic susceptibility testing by a standardized single disc method. Am J clin pathol 45(4):493–496
12. Chae A, Choi Y, Jo S, Paoprasert P, Park SY, In I (2017) Microwave-assisted synthesis of fluorescent carbon quantum dots from an A 2/B 3 monomer set. RSC Adv 7(21):12663–12669
13. Chandra S, Pathan SH, Mitra S, Modha BH, Goswami A, Pramanik P (2012) Tuning of photoluminescence on different surface functionalized carbon quantum dots. RSC Adv 2(9):3602–3606
14. Chen B, Li F, Li S, Weng W, Guo H, Guo T, Zhang X, Chen Y, Huang T, Hong X (2013) Large scale synthesis of photoluminescent carbon nanodots and their application for bioimaging. Nanoscale 5(5):1967–1971
15. CLSI (2012) Methods for Dilution Antimicrobial Susceptibility Tests for Bacteria That Grow Aerobically; Approved Standard—Ninth Edition, Vol. 32 No. 2. M07-A9 Clinical and Laboratory Standards Institute USA
16. Dasgupta S, Das B, Li Q, Wang D, Baby TT, Indris S, Knapp M, Ehrenberg H, Fink K, Kruk R (2016) Toward On-and-Off Magnetism: Reversible Electrochemistry to Control Magnetic Phase Transitions in Spinel Ferrites. Adv Func Mater 26(41):7507–7515
17. Delhaes P (2000) Polymorphism of carbon. Graphite and precursors Gordon & Breach:1–24
18. Dong X, Liang W, Meziani MJ, Sun Y-P, Yang L (2020) Carbon dots as potent antimicrobial agents. Theranostics 10(2):671
19. Du L, He G, Gong Y, Yuan WZ, Wang S, Yu C, Liu Y, Wei C (2018) Efficient persistent room temperature phosphorescence achieved through Zn2 + doped sodium carboxymethyl cellulose composites. Composites Communications 8:106–110
20. El-Naggar ME, Hasanin M, Youssef AM, Aldalbahi A, El-Newehy MH, Abdelhameed RM (2020a) Hydroxyethyl cellulose/bacterial cellulose cryogel dopped silver@ titanium oxide nanoparticles: Antimicrobial activity and controlled release of Tebuconazole fungicide. Int J Biol Macromol 165:1010–1021
21. El-Naggar ME, Hasanin M, Youssef AM, Aldalbahi A, El-Newehy MH, Abdelhameed RMJIJoBM (2020b) Hydroxyethyl cellulose/bacterial cellulose cryogel dopped silver@ titanium oxide nanoparticles: Antimicrobial activity and controlled release of Tebuconazole fungicide. 165:1010–1021
22. Emam HE, Abdelhameed RM (2017) Anti-UV radiation textiles designed by embracing with nano-MIL (Ti, In)–metal organic framework. ACS Appl Mater Interfaces 9(33):28034–28045
23. Emam HE, Abdelhamid HN, Abdelhameed RM (2018a) Self-cleaned photoluminescent viscose fabric incorporated lanthanide-organic framework (Ln-MOF). Dyes Pigm 159:491–498

24. Emam HE, Abdellatif FH, Abdelhameed RM (2018b) Cationization of celluloisc fibers in respect of liquid fuel purification. J Clean Prod 178:457–467
25. Emam HE, Ahmed HB, Gomaa E, Helal MH, Abdelhameed RM (2020a) Recyclable photocatalyst composites based on Ag 3 VO 4 and Ag 2 WO 4@ MOF@ cotton for effective discoloration of dye in visible light. Cellulose:1–17
26. Emam HE, Bechtold T (2015) Cotton fabrics with UV blocking properties through metal salts deposition. Appl Surf Sci 357:1878–1889
27. Emam HE, darwesh om, Abdelhameed RM (2020b) Protective Cotton Textiles via Amalgamation of Cross-linked Zeolitic Imidazole Framework. Industrial & Engineering Chemistry Research
28. Emam HE, Saleh N, Nagy KS, Zahran M (2016) Instantly AgNPs deposition through facile solventless technique for poly-functional cotton fabrics. Int J Biol Macromol 84:308–318
29. Emam HE, Zahran M, Ahmed HB (2017) Generation of biocompatible nanogold using H2O2–starch and their catalytic/antimicrobial activities. Eur Polymer J 90:354–367
30. Gao J, Zhu M, Huang H, Liu Y, Kang Z (2017) Advances, challenges and promises of carbon dots. Inorganic Chemistry Frontiers 4(12):1963–1986
31. Gao X, Du C, Zhuang Z, Chen W (2016) Carbon quantum dot-based nanoprobes for metal ion detection. Journal of Materials Chemistry C 4(29):6927–6945
32. Hasanin MS, Moustafa GO (2020) New potential green, bioactive and antimicrobial nanocomposites based on cellulose and amino acid. Int J Biol Macromol 144:441–448
33. Hewson M (1994) Formaldehyde in textiles. J Soc Dyers Colour 110(4):140–142
34. Ipe BI, Lehnig M, Niemeyer CM (2005) On the generation of free radical species from quantum dots. Small 1(7):706–709
35. Khan MZ, Ashraf M, Hussain T, Rehman A, Malik MM, Raza ZA, Nawab Y, Zia Q (2015) In situ deposition of TiO 2 nanoparticles on polyester fabric and study of its functional properties. Fibers Polym 16(5):1092–1097
36. Kien Nguyen T, Park K-H, Kwon PY (2016) Experimental results on lamellar-type solid lubricants in enhancing minimum quantity lubrication machining. Journal of Manufacturing Science and Engineering 138 (10)
37. Kim C, Ji T, Eom JB (2018) Determination of organic compounds in water using ultraviolet LED. Meas Sci Technol 29(4):045802
38. Kim YJ, Guo P, Schaller RD (2019) Aqueous Carbon Quantum Dot-Embedded PC60-PC61BM Nanospheres for Ecological Fluorescent Printing: Contrasting Fluorescence Resonance Energy-Transfer Signals between Watermelon-like and Random Morphologies. The Journal of Physical Chemistry Letters 10(21):6525–6535
39. Kováčová M, Špitalská E, Markovic Z, Špitálský Z (2020) Carbon Quantum Dots As Antibacterial Photosensitizers and Their Polymer Nanocomposite Applications. Part Part Syst Charact 37(1):1900348

40. Kováčová Mr, Marković ZM, Humpolíček P, Mičušík M, Švajdlenková H, Kleinová A, Danko M, Kubát P, Vajďák J, Capakova Z (2018) Carbon quantum dots modified polyurethane nanocomposite as effective photocatalytic and antibacterial agents. ACS Biomaterials Science Engineering 4(12):3983–3993
41. Li H, Huang J, Song Y, Zhang M, Wang H, Lu F, Huang H, Liu Y, Dai X, Gu Z (2018) Degradable carbon dots with broad-spectrum antibacterial activity. ACS Appl Mater Interfaces 10(32):26936–26946
42. Li H, Ming H, Liu Y, Yu H, He X, Huang H, Pan K, Kang Z, Lee S-T (2011a) Fluorescent carbon nanoparticles: electrochemical synthesis and their pH sensitive photoluminescence properties. New J Chem 35(11):2666–2670
43. Li M, Yu C, Hu C, Yang W, Zhao C, Wang S, Zhang M, Zhao J, Wang X, Qiu J (2017) Solvothermal conversion of coal into nitrogen-doped carbon dots with singlet oxygen generation and high quantum yield. Chem Eng J 320:570–575
44. Li X, Ye J, Lin Y, Fan L, Pang H, Gong W, Ning G (2011b) Facile synthesis and flame retardant performance of NaAl (OH) 2CO3 whiskers. Powder technology 206(3):358–361
45. Li YJ, Harroun SG, Su YC, Huang CF, Unnikrishnan B, Lin HJ, Lin CH, Huang CC (2016) Synthesis of self-assembled spermidine-carbon quantum dots effective against multidrug-resistant bacteria. Advanced Healthcare Materials 5(19):2545–2554
46. Liu X, Pang J, Xu F, Zhang X (2016) Simple approach to synthesize amino-functionalized carbon dots by carbonization of chitosan. Scientific reports 6:31100
47. Lu J, Yang J-x, Wang J, Lim A, Wang S, Loh KP (2009) One-pot synthesis of fluorescent carbon nanoribbons, nanoparticles, and graphene by the exfoliation of graphite in ionic liquids. ACS Nano 3(8):2367–2375
48. Luo Z, Lu Y, Somers LA, Johnson AC (2009) High yield preparation of macroscopic graphene oxide membranes. J Am Chem Soc 131(3):898–899
49. Nazari A, Montazer M, Mirjalili M, Nazari S (2013) Polyester with durable UV protection properties through using nano TiO2 and polysiloxane softener optimized by RSM. Journal of The Textile Institute 104(5):511–520
50. Perego P, Moltani A, Andreoni G Sport monitoring with smart wearable system. In: pHealth (2012) pp 224–228
51. Phung Hai TA, Sugimoto R (2017) Photoluminescence control of cellulose via surface functionalization using oxidative polymerization. Biomacromol 18(12):4011–4021
52. Pierson H (1993) Handbook of Carbon, Graphite, Diamond, and Fullerenes: Properties, Processing and Applications, Noyes, Park Ridge
53. Pires NR, Santos CM, Sousa RR, Paula R, Cunha PL, Feitosa J (2015) Novel and fast microwave-assisted synthesis of carbon quantum dots from raw cashew gum. J Braz Chem Soc 26(6):1274–1282
54. Rehan M, Hartwig A, Ott M, Gätjen L, Wilken R (2013) Enhancement of photocatalytic self-cleaning activity and antimicrobial properties of poly (ethylene terephthalate) fabrics. Surface Coatings

Technology 219:50–58

55. Ristic BZ, Milenkovic MM, Dakic IR, Todorovic-Markovic BM, Milosavljevic MS, Budimir MD, Paunovic VG, Dramicanin MD, Markovic ZM, Trajkovic VS (2014) Photodynamic antibacterial effect of graphene quantum dots. Biomaterials 35(15):4428–4435
56. Sahin O, Kayacan O, Bulgun EY (2005) Smart textiles for soldier of the future. Defence Science Journal 55(2):195
57. Sakaki T, Shibata M, Miki T, Hirosue H, Hayashi N (1996) Reaction model of cellulose decomposition in near-critical water and fermentation of products. Biores Technol 58(2):197–202
58. Sakthivel M, Drillet J-F (2018) An extensive study about influence of the carbon support morphology on Pt activity and stability for oxygen reduction reaction. Appl Catal B 231:62–72
59. Salama A, Hasanin M, Hesemann PJCP (2020) Synthesis and antimicrobial properties of new chitosan derivatives containing guanidinium groups.116363
60. Shao X, Wu W, Wang R, Zhang J, Li Z, Wang Y, Zheng J, Xia W, Wu M (2016) Engineering surface structure of petroleum-coke-derived carbon dots to enhance electron transfer for photooxidation. J Catal 344:236–241
61. Song J, Zhao L, Wang Y, Xue Y, Deng Y, Zhao X, Li Q (2018) Carbon quantum dots prepared with chitosan for synthesis of CQDs/AuNPs for iodine ions detection. Nanomaterials 8(12):1043
62. Stanković NK, Bodik M, Šiffalovič P, Kotlar M, Mičušik M, Špitalsky Z, Danko M, Milivojević DaD, Kleinova A, Kubat P (2018) Antibacterial and antibiofouling properties of light triggered fluorescent hydrophobic carbon quantum dots Langmuir–Blodgett thin films. ACS Sustainable Chemistry Engineering 6(3):4154–4163
63. Tao X, Koncar V, Huang T-H, Shen C-L, Ko Y-C, Jou G-T (2017) How to make reliable, washable, and wearable textronic devices. Sensors 17(4):673
64. Welch CM (1988) Tetracarboxylic acids as formaldehyde-free durable press finishing agents: part I: catalyst, additive, and durability studies. Text Res J 58(8):480–486
65. Wissler M (2006) Graphite and carbon powders for electrochemical applications. Journal of power sources 156(2):142–150
66. Wu ZL, Gao MX, Wang TT, Wan XY, Zheng LL, Huang CZ (2014) A general quantitative pH sensor developed with dicyandiamide N-doped high quantum yield graphene quantum dots. Nanoscale 6(7):3868–3874
67. Yang CQ, Chen D, Guan J, He Q (2010) Cross-linking cotton cellulose by the combination of maleic acid and sodium hypophosphite. 1. Fabric wrinkle resistance. Ind Eng Chem Res 49(18):8325–8332
68. Yang CQ, Xu L, Li S, Jiang Y (1998) Nonformaldehyde durable press finishing of cotton fabrics by combining citric acid with polymers of maleic acid. Text Res J 68(6):457–464
69. Zhang H, Wang H, Chen G (2006) A new kind of conducting filler-graphite nano sheets. Plastics 35(4):42–50

70. Zhang J, Bao L, Lou H, Deng J, Chen A, Hu Y, Zhang Z, Sun X, Peng H (2017a) Flexible and stretchable mechanoluminescent fiber and fabric. Journal of Materials Chemistry C 5(32):8027–8032
71. Zhang P, Lan J, Wang Y, Huang CZ (2015) Luminescent golden silk and fabric through in situ chemically coating pristine-silk with gold nanoclusters. Biomaterials 36:26–32
72. Zhang Z, Shi X, Lou H, Xu Y, Zhang J, Li Y, Cheng X, Peng H (2017b) A stretchable and sensitive light-emitting fabric. Journal of Materials Chemistry C 5(17):4139–4144
73. Zuo J, Jiang T, Zhao X, Xiong X, Xiao S, Zhu Z (2015) Preparation and application of fluorescent carbon dots. Journal of Nanomaterials 2015

## Supplemental Table

Table S1 was is not available with this version.

## Figures

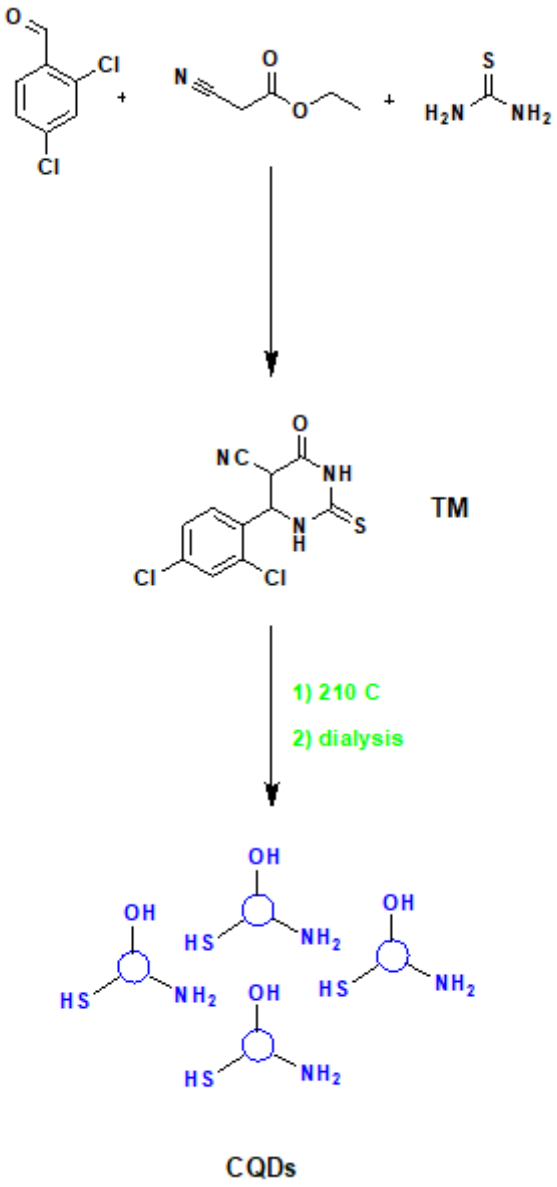


## Figure 1

The preparation scheme for TM and CQDs.

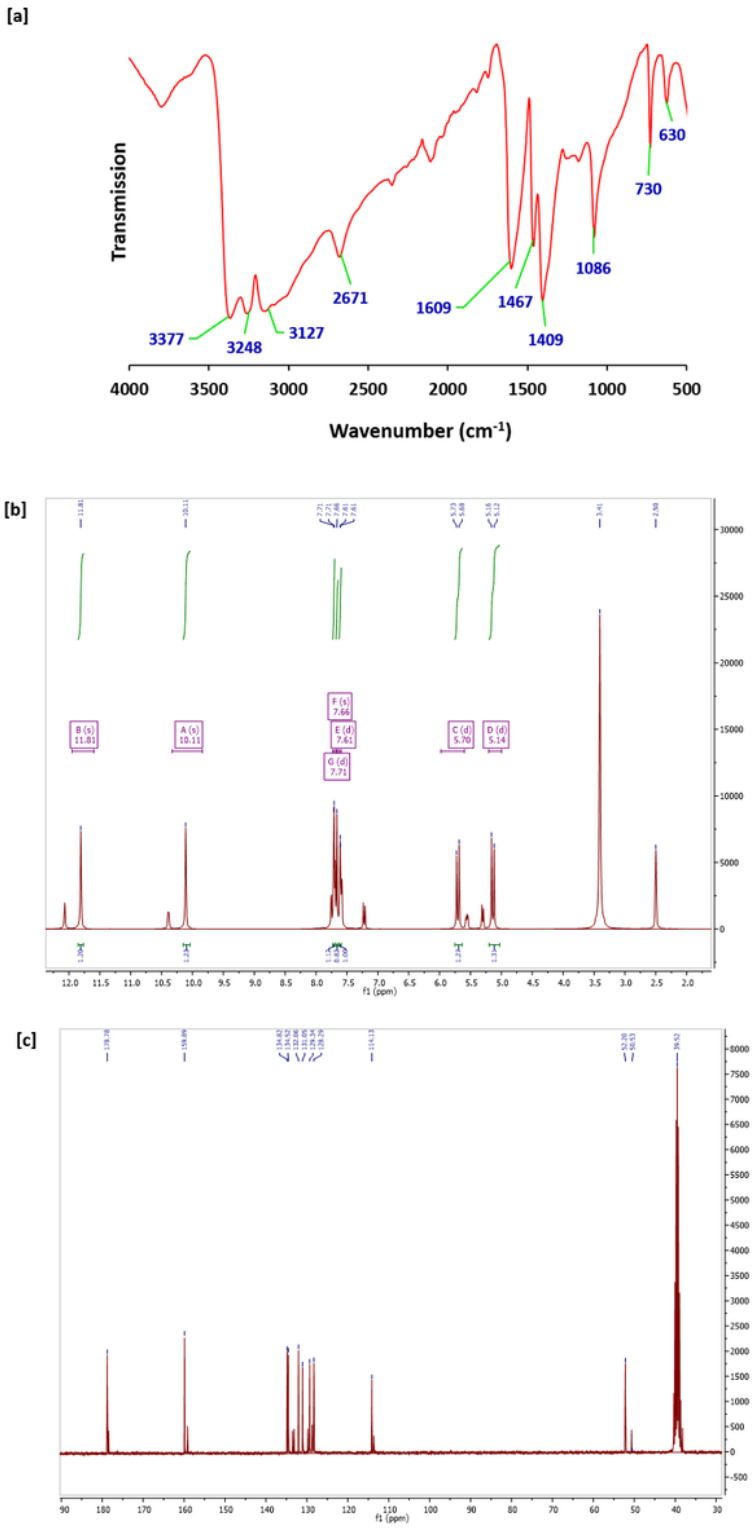


## Figure 2

Spectral data for target molecule; [a] infrared spectra, [b] 1HNMR spectra and [c] 13CNMR.

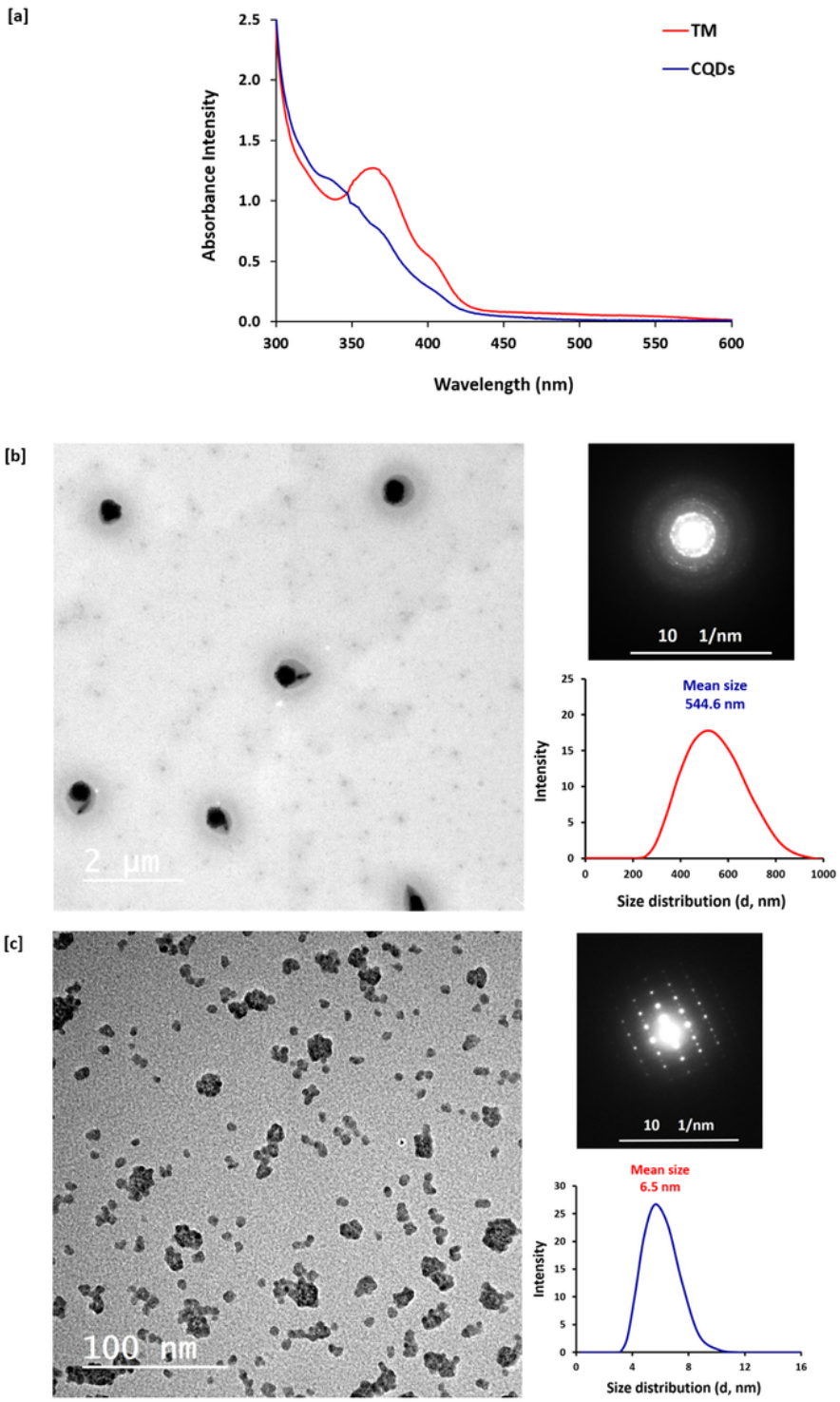


## Figure 3

[a] UV-Visible absorbance spectra, [b] TEM micrograph for target molecule and [c] TEM micrograph for CQDs. Size distribution from zetasizer and patterns are include in the corresponding micrographs.

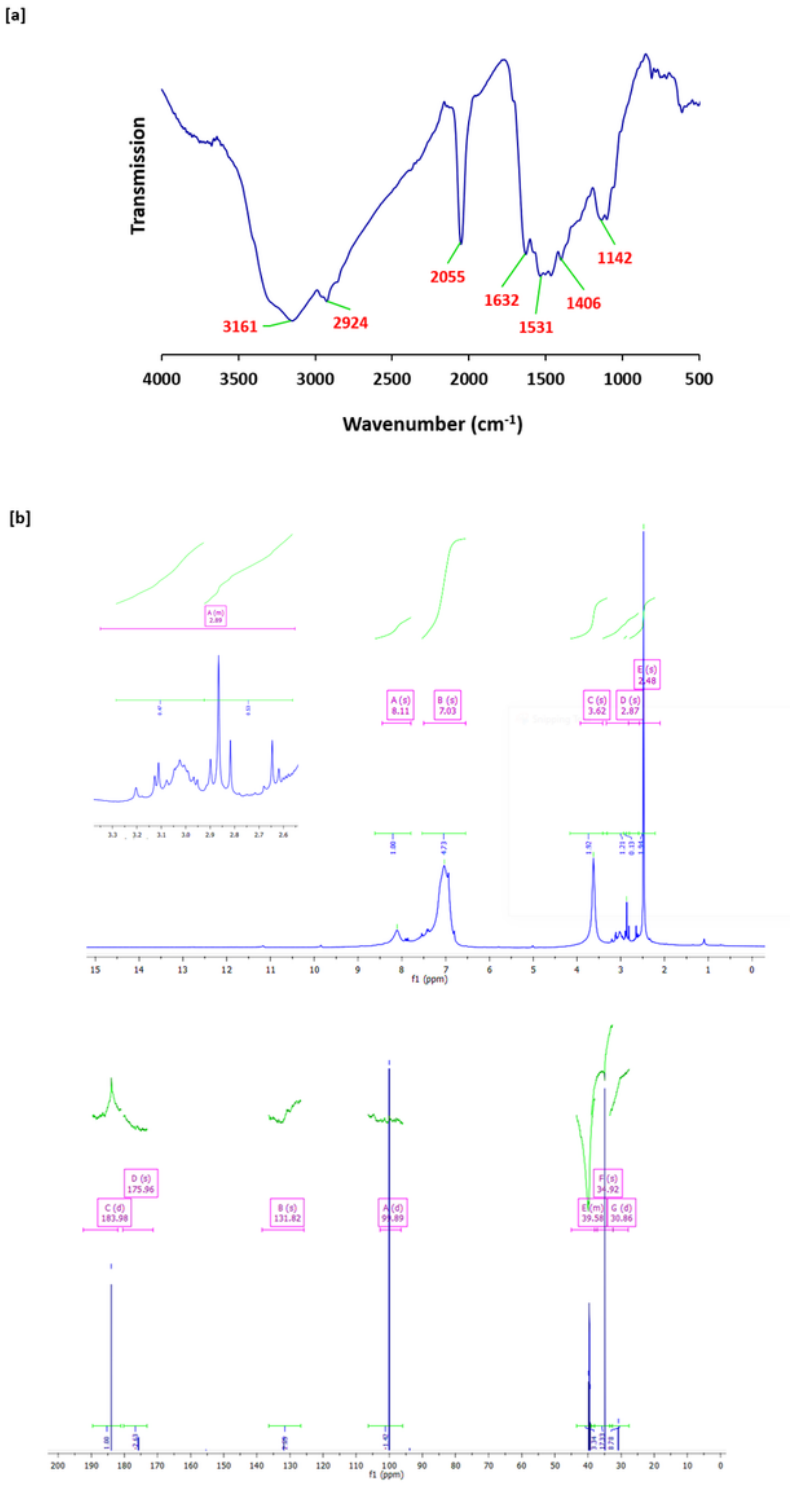


## Figure 4

Spectral data for the synthesized carbon nanostructures; [a] Infrared spectra, [b] 1HNMR spectra and [c] 13CNMR.

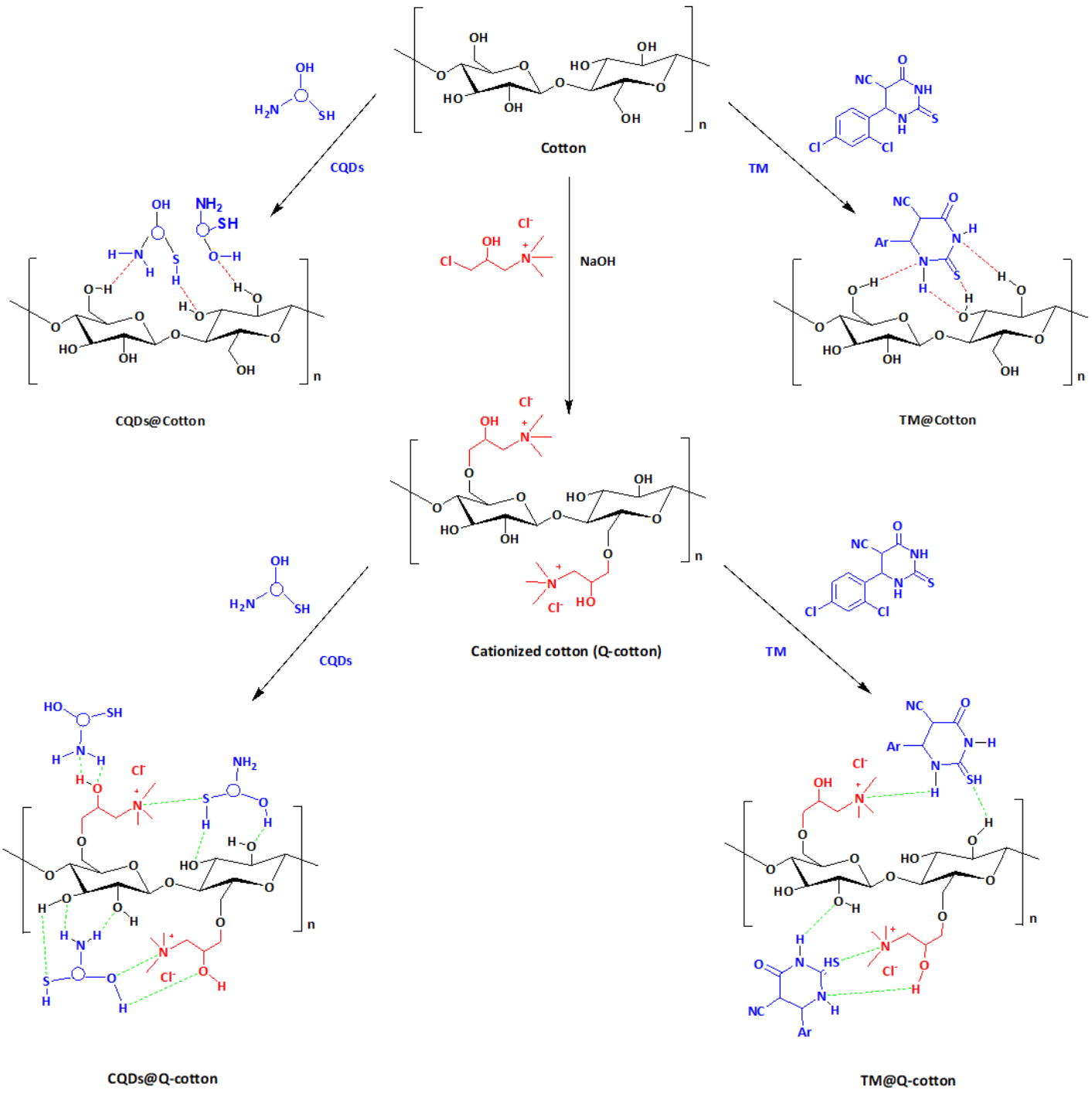


## Figure 5

The preparation mechanism for modified cotton fabrics.

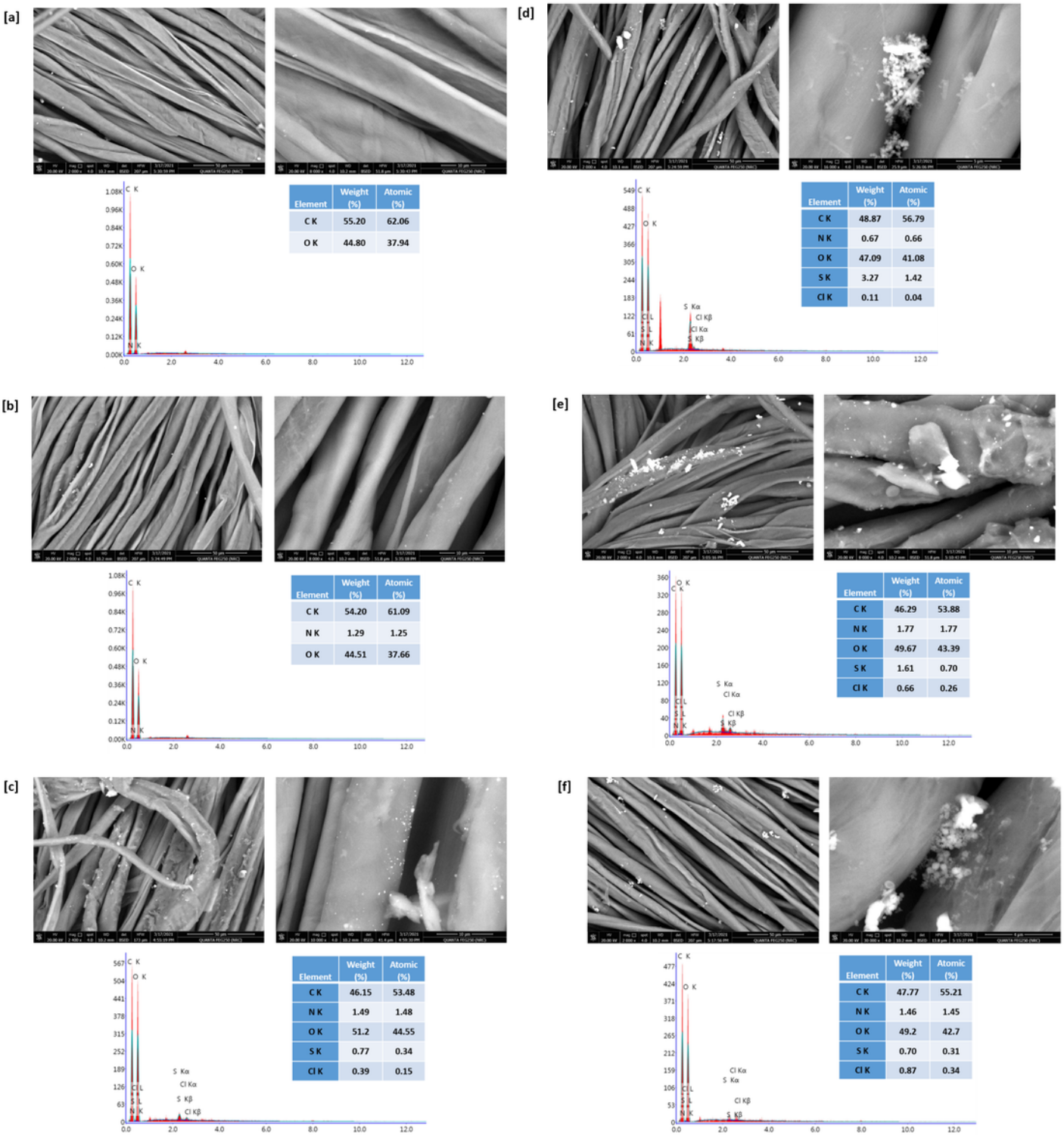


## Figure 6

Microscopic images and EDX analyses for modified fabrics; [a] cotton, [b] Q-cotton [c] TM@cotton, [d] CQDs@cotton, [e] TM@cationized cotton and [f] CQDs@cationized cotton.

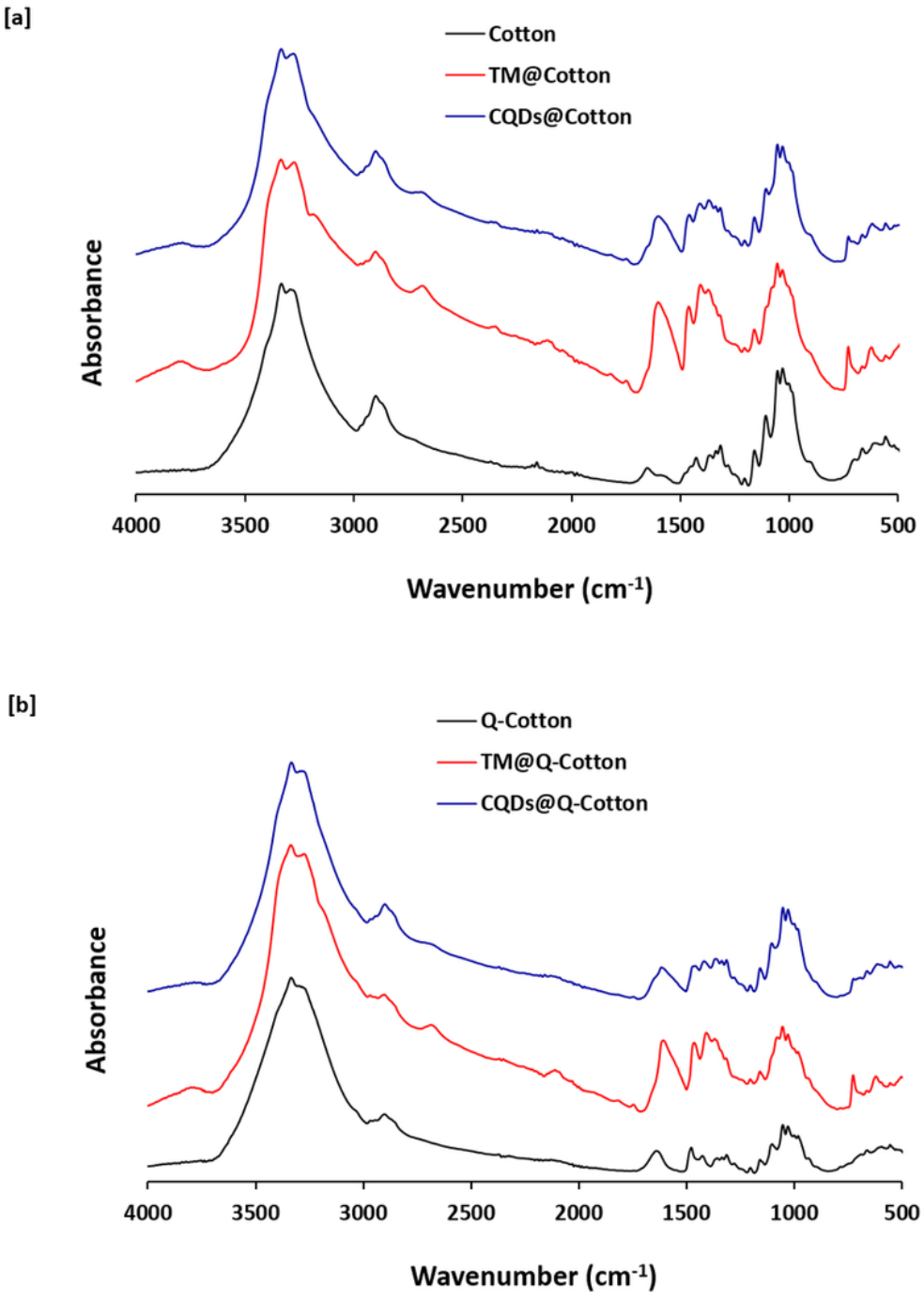


## Figure 7

FTIR for modified fabrics; [a] modified cotton and [b] modified cationized cotton.

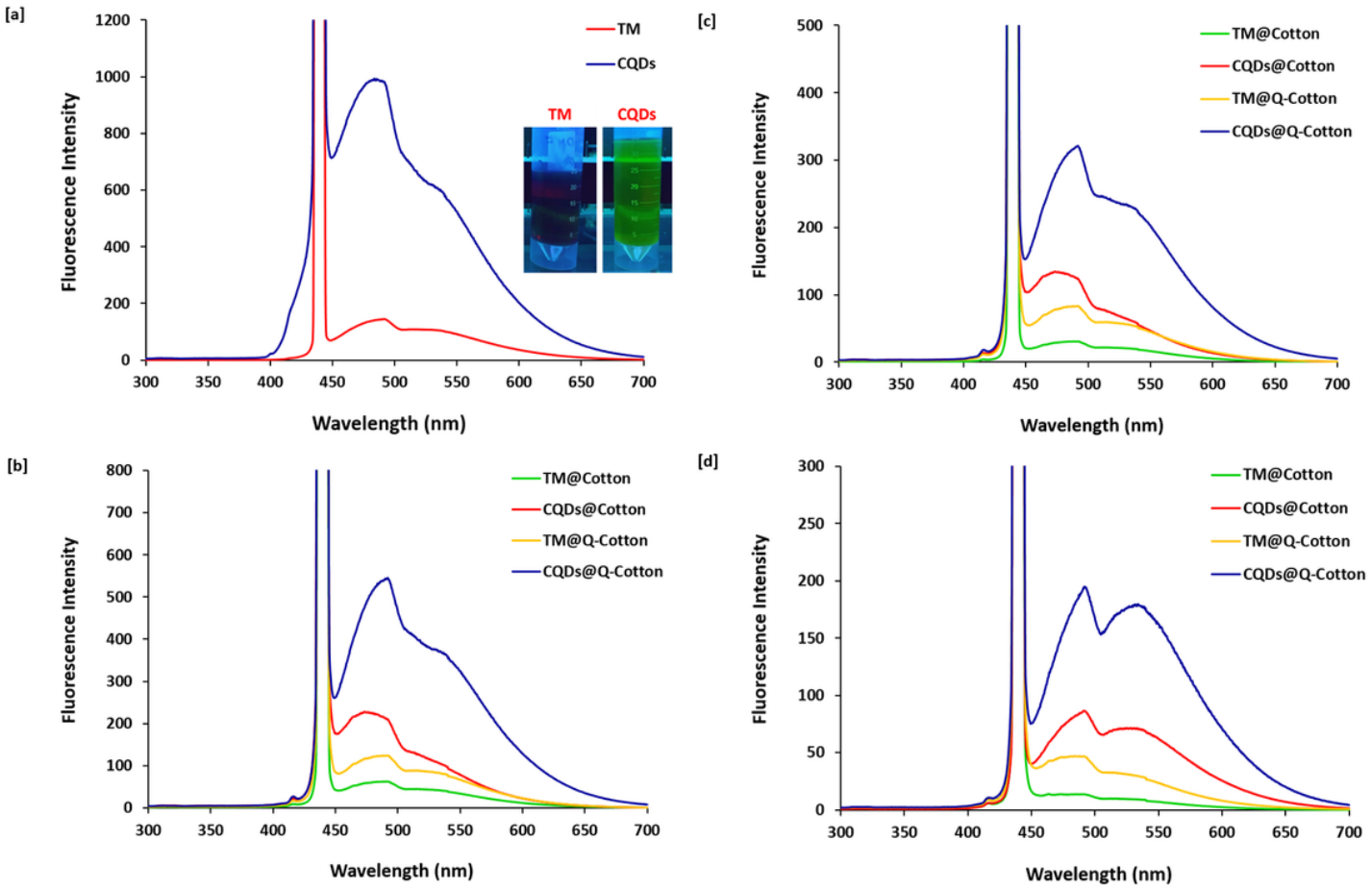


## Figure 8

Emission spectra at room temperature for; [a] solutions (inset, image under the UV-lamp), [b] modified cotton and [c] modified cotton after 5 washings. The excitation carried out at 440 nm.

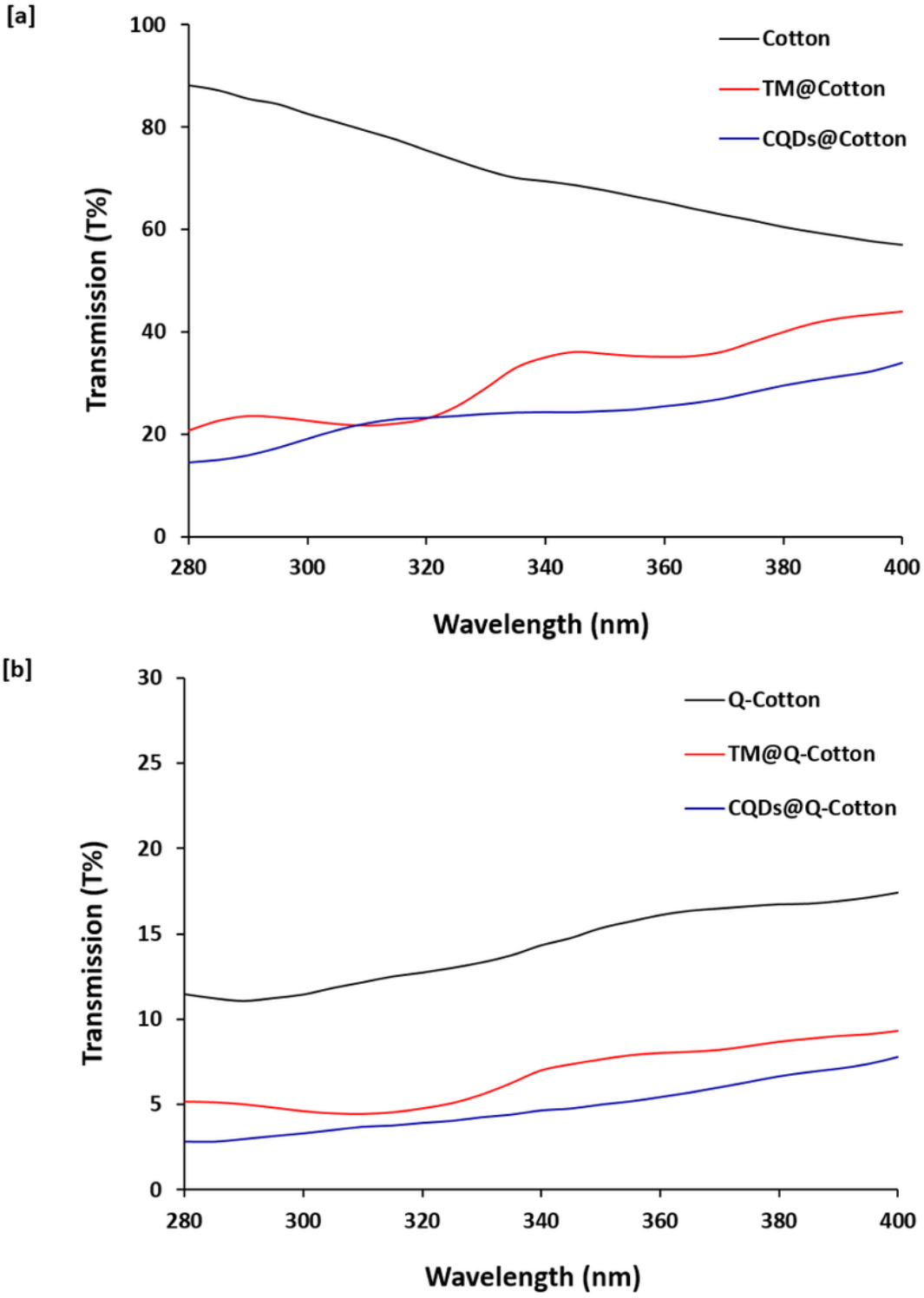


**Figure 9**

Transmission through the treated fabrics; [a] modified cotton and [b] modified cationized cotton.

# Supplementary Files

This is a list of supplementary files associated with this preprint. Click to download.

- GraphicalAbstract.docx
- Supplementaryfile.docx